International Journal of Control and Automation
Vol.9, No.1 (2016), pp.241-250
http://dx.doi.org/10.14257/ijca.2016.9.1.22

Hydraulic Quadruped Robot Joint Force Control Based on Double Internal Model Controller

Zhongwen Wang[1], Ruizhen Duan[1], Guitao Sun [2] and Mingshan Chi[1]

[1] *Rongcheng College; Harbin University of Science and Technology, Shandong, 264300, P.R. China*
[2] *Mechanical & Power Engineering College; Harbin University of Science and Technology, Harbin 150080; P.R. China*
wangzhongwen1979@qq.com

Abstract

In order to improve the servo accuracy of hydraulic quadruped robot electro-hydraulic servo actuators during operation, the load characteristic of equivalent model of electro-hydraulic servo actuators with swing phase and support phase was analyzed, respectively, the compound control strategy including flow compensator, velocity compensator, internal model controller, and improved internal model controller was proposed, the dynamic performance of system was guaranteed by internal model controller, the accuracy was further improvement by improved internal model controller. The composite control strategy was verified by robot single leg test platform, the experiment results show that the deviation and phase lag of response curve with flow compensation, velocity compensation and internal model controller was less than ±5% and 18°, respectively, the value of phase lag can be further reduced to 7°by the improved internal model controller, and the efficiency of the proposed control strategy was verified.

Keywords: *hydraulic quadruped robot, electro-hydraulic force servo, flow compensation, velocity compensation, internal model control, minimal control synthesis*

1. Introduction

Hydraulic Quadruped Robot uses the electro-hydraulic servo actuator as the driving element, indirectly through the piston rod out or in to drive the each joint rotation. Accurate control of actuators is the basis and prerequisite of the stable operation of the robots, especially in support of joint force control, the controller directly affect the precision of robot operation stability. However, in view of the electro-hydraulic servo actuator force control research has a lot of achievements, such as nonlinear robust force control [1] , quantitative feedback step[2], nonlinear adaptive inverse control[3], neural network[4], genetic algorithm [5], the adaptive fuzzy control [6], the iterative learning method and force control based on state observer [7-8]. But the above research objects are all on the same model of the structure of the fixed parameter or variable parameter model, the force control model structure and the system operating mode of the hydraulic actuators robot are time-varying model parameters. The multiple model method is the better way to solve the model structure is different, but it can't guarantee controller system stability in the process of switching [9].

Therefore, aiming at the shortcomings of the above research, based on the hydraulic characteristics of quadruped robot, this paper first analyze the equivalent model of hydraulic robot electro-hydraulic servo actuator in the swing phase, rigid support and elastic support phase. Secondly, based on the model characteristics, this paper proposes a compound control strategy of the servo valve flow compensation, compensation system speed, and internal model controller and improve the internal model controller applying the inner ring internal model controller to improve the dynamic characteristics of system.

ISSN: 2005-4297 IJCA

Finally, this paper uses a single robot leg to test the compound control strategy for rigid support and elastic support in order to illustrate the effectiveness of the proposed control strategy.

2. Mode of the Electro-Hydraulic Servo Actuator

The one leg structure of the hydraulic driving quadruped robot is shown in figure 1. The actuator equivalent models of the legs in the swing phase, rigid support phase and elastic support phase, which are deduced in [10], are shown in figure 2 a), b) and c).

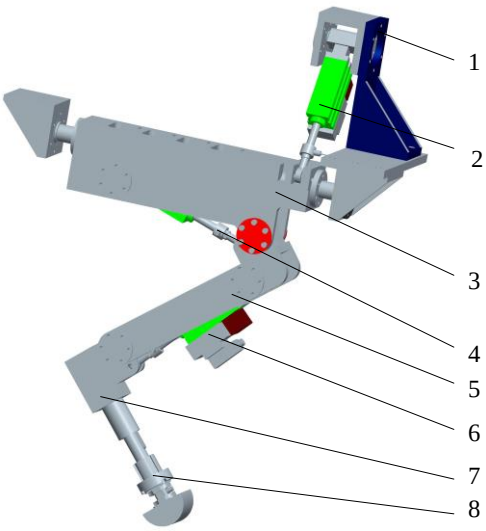

1) frame, 2) horizontal pendulum actuator, 3) link, 4) knee joint actuator, 5) link Ⅱ,6) hip joint actuator, 7) link Ⅲ, 8) link Ⅳ

Figure 1. Single Structure Of Quadruped Robot

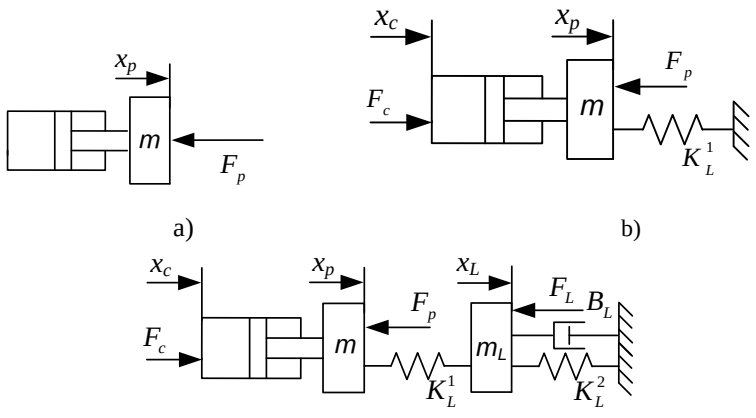

a) b)

c)

Figure 2. Actuator Equivalent Model

The force balance equations of the hydraulic cylinder and the load in the swing phase, rigid support phase and the elastic support phase are shown as below respectively

$$A_1 p_L = m\ddot{x}_p + B_p\dot{x}_p + F_p \quad (1)$$

A_1 is the area of hydraulic cylinder rodless cavity, p_L is the load pressure, $p_L=p_1-p_2$, p_1 is the pressure of the hydraulic cylinder rodless cavity, p_2 is the pressure of the hydraulic cylinder rod cavity, n is the area ratio of the rod cavity and rodless cavity, B_p is the friction coefficient.

$$\begin{cases} A_1 p_L = m\ddot{x}_p + B_p(\dot{x}_p - \dot{x}_c) + K_L^1 x_p + F_p \\ A_1 p_L = -m_c\ddot{x}_c + B_p(\dot{x}_p - \dot{x}_c) + F_c \end{cases} \tag{2}$$

$$\begin{cases} A_1 p_L = m\ddot{x}_p + B_p(\dot{x}_p - \dot{x}_c) + K_L^1(x_p - x_L) + F_p \\ K_L^1(x_p - x_L) = m_L\ddot{x}_L + B_L\dot{x}_L + K_L^2 x_L + F_L \\ A_1 p_L = -m_c\ddot{x}_c + B_p(\dot{x}_p - \dot{x}_c) + F_c \end{cases} \tag{3}$$

In the support phase, due to the displacement sensor can only test relative displacement of the piston rod and cylinder, X_p - X_c, suppose $X = X_p$-X_c,

$$AA(\mathrm{s}) = mm_c\,\mathrm{s}^4 + (m+m_c)B_p\,\mathrm{s}^3 + m_c K_L^1\,\mathrm{s}^2 + B_p K_L^1 s,$$

$$BB(\mathrm{s}) = ms^2 + \frac{(m_L s^2 + B_L s + K_L^2)K_L^1}{m_L s^2 + B_L s + K_L^1 + K_L^2}, \qquad CC(\mathrm{s}) = (m+m_c)\mathrm{s}^2 + K_L^1$$

Due to the servo valve frequency is higher, it can be simplified as proportion link, the simplified transfer function of servo valve can be expressed as

$$\frac{X_V}{\Delta I} = K_{xv} \tag{4}$$

X_V is the displacement of servo valve core, K_{xv} is the gain of servo valve, ΔI is the incoming current of servo valve.

By the literatures [11-12], the actuator force control block diagrams are shown in figure 3 a), b) and c), which are obtained from the equation (1), (2), (3) and (4) respectively in the swing phase and the rigid support and elastic support phase.

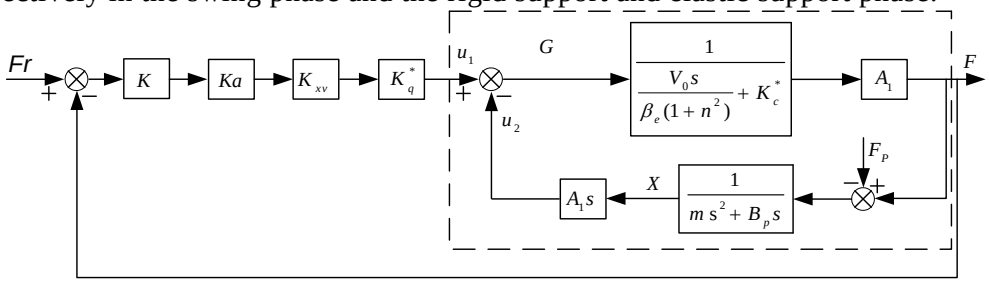

a)

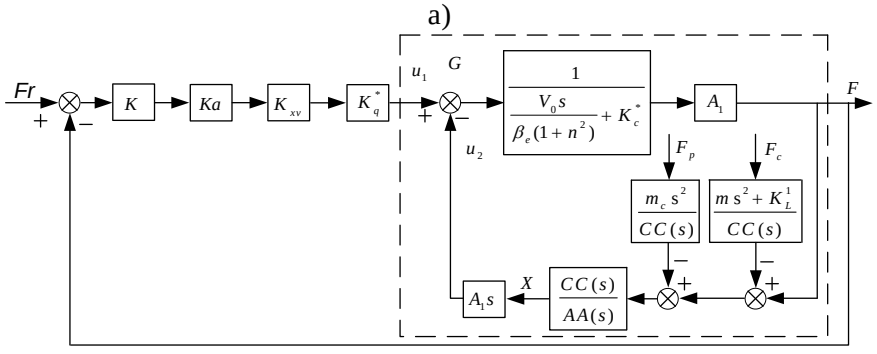

b)

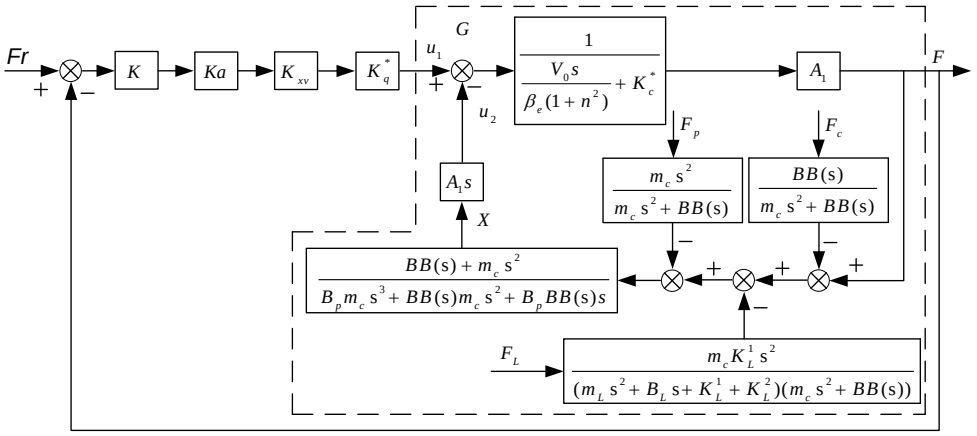

c)

Figure 3. Diagram of electro-hydraulic Force Servo System

When $X_V > 0$,

$$K_q^* = C_d w \sqrt{\frac{1}{\rho}} \cdot \sqrt{\frac{2}{1+n^3}} \cdot \sqrt{p_s - p_L}$$

C_d is the flow coefficient of servo valve, w is the area gradient of servo valve, ρ is the density of hydraulic oil, p_s is the oil supply pressure.

When $X_V < 0$,

$$K_q^* = C_d w \sqrt{\frac{1}{\rho}} \cdot \sqrt{\frac{2}{1+n^3}} \cdot \sqrt{nP_s + P_L}$$

K_q^* is the pressure coefficient of the servo valve.,

When $X_V > 0$,

$$K_c^* = C_d w X_V \sqrt{\frac{1}{\rho}} \cdot \frac{1}{2} \cdot \sqrt{\frac{2}{1+n^3}} \cdot \frac{1}{\sqrt{\frac{(1+n)p_s}{2}}}$$

When $X_V \leqslant 0$,

$$K_c^* = \frac{C_d w X_V}{2} \cdot \sqrt{\frac{1}{\rho}} \cdot \sqrt{\frac{2}{1+n^3}} \cdot \frac{1}{\sqrt{nP_s + P_L}}$$

3. Design of Controller

Figure 4 is a block diagram of compound control strategy. *G* is dotted box in figure 3, *FLC* is the flow compensator, *VC* is the speed compensator, *IMC* is the internal model controller, G_{a2}^{-1} is the internal model controller introducing the inverse model of the filter, α is the adjustable coefficient between 0 ~ 1, G_{a2}^{-1}、 *PG* and α compose the improved internal model control structure.

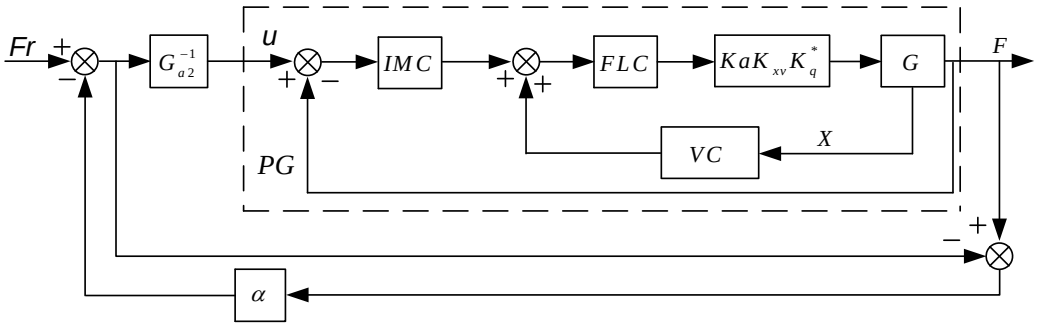

Figure 4. Principle Diagram of Compound Controller

3.1 Flow Speed Compensator

Equivalent gain of servo valve is

$$\frac{Q_{n1}K_a}{I_n\sqrt{\Delta P_n}}\sqrt{\frac{\lambda p_s}{1+n^3}} \tag{5}$$

The structure of the speed compensator is

$$VC=\frac{A_1 s}{\frac{Q_{n1}K_a}{I_n\sqrt{\Delta P_n}}\sqrt{\frac{\lambda p_s}{1+n^3}}} \tag{6}$$

After the flow compensation and speed compensation, the equivalent force control block diagram is shown in figure 5.

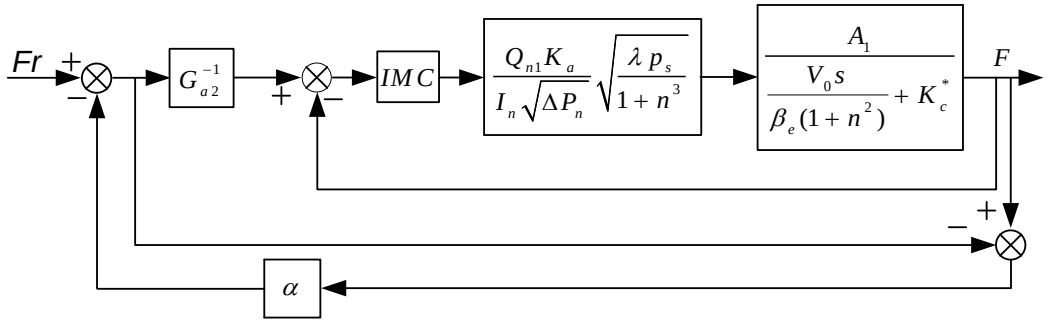

Figure 5. Equivalent Diagram of Force Control

Suppose $K_V=\frac{Q_{n1}K_aA_1}{K_c^*I_n\sqrt{\Delta P_n}}\sqrt{\frac{\lambda p_s}{1+n^3}}$, $\frac{1}{\omega_r}=\frac{V_0}{\beta_e(1+n^2)K_c^*}$

The open loop transfer function of the system is

$$KK_V\Big/\frac{1}{\omega_r}s+1 \tag{7}$$

After the flow compensation and speed compensation, the system eliminates the quality equivalent load and equivalent spring stiffness influencing the performance of the system and the model structure is the first order inertia link.

3.2 Internal Model Control

Internal model control principle diagram is shown in figure 6, *d* is the jamming signal, *Q* (*s*) is the internal model controller, *M* (*s*) is the mathematical model of controlled object, *C* (*s*)is the feedback controller, *P* (*s*) is the actual controlled object, *D* (*s*) shows the effect of interference on the output.

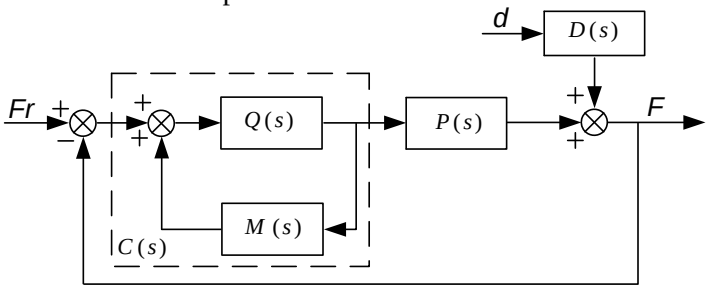

Figure 6. Principle Diagram of Internal Model Control

From figure 6, the system output is shown in equation (8).

$$F = \frac{Q(s)P(s)Fr}{1+Q(s)[P(s)-M(s)]} + \frac{[1-Q(s)M(s)]D(s)d}{1+Q(s)[P(s)-M(s)]} \quad (8)$$

In equation (8), when the relation between internal model controller and the system model meets the equation (9), it can realize zero phase tracking and interference suppression of the system.

$$Q(s) = M(s)^{-1} \quad (9)$$

In order to obtain the real-time parameters of the controlled object model, it usually use the online identification method, but from the online identification models can't guarantee a certain for non-minimum phase system and be easy to cause the system unstable. The identification methods in this paper adapt the least square method according to reference [13].

Introducing the filer,

$$1/\sigma s+1 \quad (10)$$

σ is the filter time constant in the equation 10.

Supposing the identification model is *M* (*s*), the relation between the actual controlled object *P* (*s*) and the model *M* (*s*) is

$$P(s) = M(s)(1+\Delta P(s)) \quad (11)$$

ΔP (*s*) is the un-modeled item.

The closed loop transfer function of the system can be expressed as

$$PG(s) = \frac{1+\Delta P(s)}{\sigma s+1+\Delta P(s)} = \frac{1}{\sigma s+1}(1+\frac{\sigma s\Delta P(s)}{\sigma s+1+\Delta P(s)}) \quad (12)$$

3.3 improved the Internal Model Control

The principle diagram of the improved internal model can be shown in figure 7[14-15]. $G_{a2}^{-1}(s)$ is the inverse model of equation 10. Due to the model is known, the $G_{a2}^{-1}(s)$ can be identified by using the offline methods.

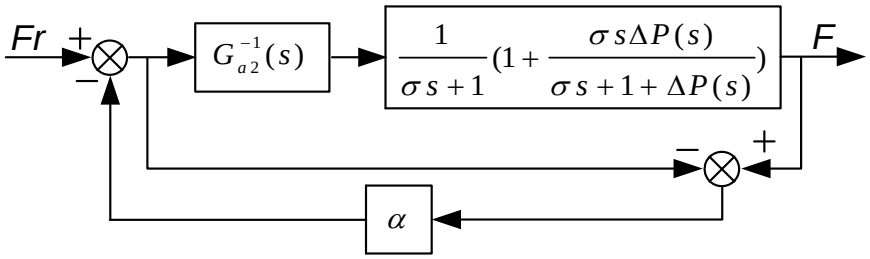

Figure 7. Improved Internal Model Control

4. Research Study

For the test platform can only realize the vertical motion, the yawing actuators in the experiment keep stationary. Figure 8 is the leg mechanism of the robot.

Considering the robot actuator executes the force control in the support phase, this paper carried out the actuator tracking experiments in the rigid support and elastic support phase respectively. Figure 9 is the leg experiment condition, a) for the rigid support phase, b) for the elastic support phase. In the figure b, 1 is the foot end, 2 is the elastomeric, used to simulate the elastic ground.

Figure 8. Leg Picture of Robot

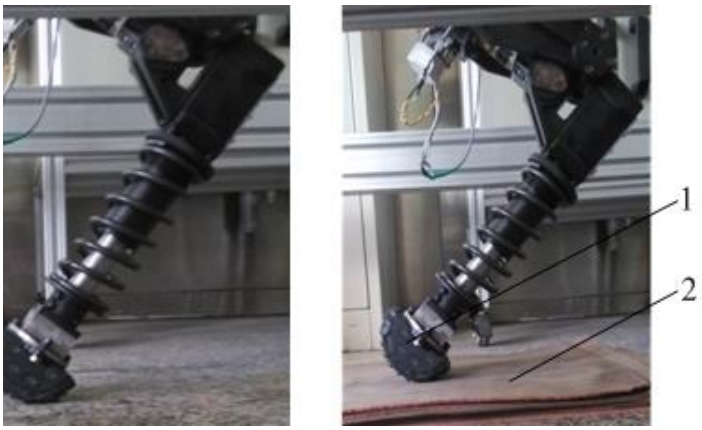

Figure 9. Condition of Experiment

In the experiment, this paper carries out the force control of hip only, through testing the output value of knee joint displacement sensor to control the knee joint angel, to ensure that the body only in the vertical direction.

Figure 10 is the force tracking curve of the hip joint in the rigid support and elastic support, the controller is PID, R is the command signal, Rp, EP are rigid support and elastic support phase force tracking curve respectively.

The figure shows that the hip joint force tracking curve response characteristics in the rigid support and elastic support are basically the same, the phase lags 36°, the amplitude deviation is within the plus or minus 5%, for the reason that the stiffness of the elastomeric is bigger than the damping spring, so it has less effect the system performance. The following paper will only study the effect of the rigid support force tracking curve.

Figure 11 is the force tracking curve introducing the internal model controller and the improved internal model controller. The figure shows that the system with the compound control strategy of the PID controller, the internal model controller and the improved internal model controller responses the deviation within ±5%, but the phase lag characteristics are different. The PID controller lags 36 ° phase, the internal model controller lags 18 ° phase, the compound controller lags 7° phase. This illustrates the effectiveness of the hybrid control strategy.

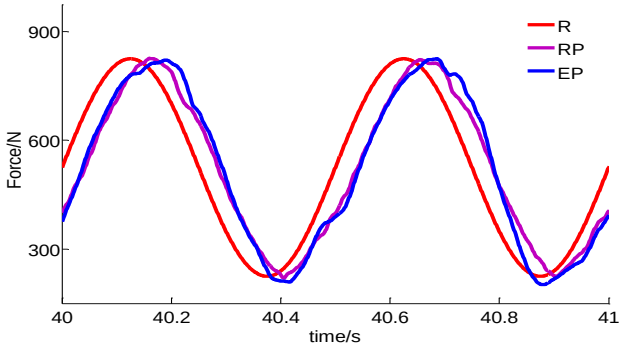

Figure 10. Force Curve of Hip Joint

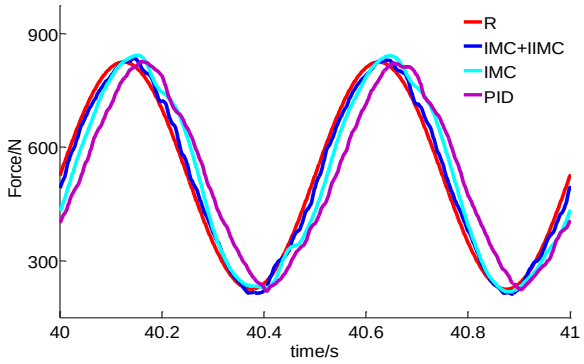

Figure 11. Force Curve with Compound Control Strategy

5. Conclusion

1) For the characteristics of electro-hydraulic servo actuator in the rigid support and elastic support phase, this paper proposed a compound control strategy of robot joint force control composed by the servo valve flow compensator, speed compensator internal model controller, inner ring and outer ring to improve internal model controller.

2) The two levels of internal model controller avoided directly calculate the inverse model of controlled object. By adjusting the improvement the adjustment coefficient of internal model controller can adjust the force the tracking error of the system.

3) The one leg testing platform shows that the hybrid control strategy can make the system amplitude deviation within the plus or minus 5%, phase lag is less than 7°, verified the effectiveness of the proposed control strategy.

Acknowledgment

This work supported by the Key Program of National Natural Science Foundation of Heilongjiang No.ZD201309, and Project supported by the Maor International Joint Research Program of China (Grant No.2013DFA71120), and the Research Program supported by the Program for New Century Excellent Talents of Heilongjiang No.1252-NCET-17.

Reference

[1] J.Y. Yao, Z.X. Jiao, B. Yao, Y.X. Shang and W.B. Dong, "Nonlinear adaptive robust force control of hydraulic load simulator", Chinese Journal of Aeronautics, vol.25, no.5, **(2012)**, pp.766-775.
[2] K. Mark and S. Nariman, "Electro-hydraulic force control design of a hardware-in-the-loop load emulator using a nonlinear QFT technique", Control engineering practice, vol.20, no.6, **(2012)**, pp.598-609.
[3] J.Y. Yao, Z.X. Jiao and B. Yao, "Nonlinear adaptive robust back stepping force control of hydraulic load simulator: theory and experiments", Journal of Mechanical Science and Technology, vol.28, no.4, **(2014)**, pp.1499-1507.
[4] M. Pisan, D. Nattawoot and Y. Yoshio, "Tuning PID controller using genetic algorithms for electro-hydraulic system with tracking force control", Advanced Materials Research, **(2014)**, pp. 1318-1322.
[5] J.Y. Li, Y.W. Wang, X.J. Wang, J.P. Shao, T.Y. Yang and Z.Y. Mao, "Research on electro-hydraulic force servo system based on neural network and fuzzy intelligent control strategy", Journal of Computational and Theoretical Nanoscience, vol.11, no.4, **(2014)**, pp.1205-1210.
[6] M.H. Chiang and H.T. Lin, "The force control of a novel variable rotational speed hydraulic pump-controlled system using adaptive fuzzy controller with self-tuning fuzzy sliding-mode compensation", IFAC Proceedings Volumes (IFAC-PapersOnline), **(2011)**, pp.968-973.
[7] M. Sun, C.C. Li and X.D. Liu, "Study on force control for fatigue testing machine based on iterative learning control", 2011 2nd International Conference on Artificial Intelligence, Management Science and Electronic Commerce, AIMSEC 2011 – Proceedings, **(2011)**, pp.4374-4378.
[8] N. Prut and K. Suwat, "Observer-based back stepping force control of an electro hydraulic actuator", Control Engineering Practice, vol.17, no.8, **(2009)**, pp.898-902.
[9] Z.J. Wang, Y.M. Fang and Y.H. Li, "Multi-model switching control for rolling mill hydraulic servo

system with input constraints" Chinese Journal of Scientific Instrument, vol.34, no.4, **(2013)**, pp.882-883.**)**

[10] J.P. Shao, G.T. Sun, B.W. Gao, W.Y. Yang and Z.H. Jin, "Hydraulic robot actuator control based on minimal control synthesis algorithm", Journal of sichuan university (Engineering science edition), vol.46, no.6, **(2014)**, pp.179-181.

[11] Z.L. Wang, "Modern electric and hydraulic servo control. Beijing university of aeronautics and astronautics press"， Beijing （**2005**）**,** pp. 16-26.

[12] H.R. Li, "Hydraulic control system", National defense industry press Beijing **(1981,** pp.229-232.

[13] T. Liu and F. Gao, "New insight into internal model control filter design for load disturbance rejection", Iet Control Theory and application, vol.4, no.3, **(2010)**, pp.448-460.

[14] G. Shen, Z.C. Zhu, Y. Tang, L. Zhang, G.D. Liu, J.S. Zhao, C.F. Yang, J.W. Han, "Combined control strategy using internal model control and adaptive inverse control for electro-hydraulic shaking table", Proceedings of the institution of mechanical engineers, Part C:journal of mechanical engineering science, vol.227, no.10, **(2013)**, pp.4-8.

[15] J. Chen and C.Y. Dong, "Nonlinear internal model control strategy based on neural network", Journal of Harbin university of science and technology, vol.9,no.1, **(2004)**, pp.17-20

